Unusual magnetic properties in Pr1−xSrxFe0.8Ni0.2O3−delta (x

Idoia Ruiz de Larramendi, R. López Antón, José I. Ruiz de Larramendi, Teófilo Rojo, Alain Wattiaux, Jesus Rodríguez Fernández

AIP Journal of Applied Physics

Unusual magnetic properties in Pr 1 − x Sr x Fe 0.8 Ni 0.2 O 3 − δ (x ≤ 0.3)

I. Ruiz de Larramendi, R. López Antón, J. I. Ruiz de Larramendi, T. Rojo, A. Wattiaux, and J. Rodríguez Fernández

Citation: Journal of Applied Physics **103**, 033902 (2008); doi: 10.1063/1.2830984
View online: http://dx.doi.org/10.1063/1.2830984
View Table of Contents: http://scitation.aip.org/content/aip/journal/jap/103/3?ver=pdfcov
Published by the AIP Publishing

Unusual magnetic properties in $Pr_{1-x}Sr_xFe_{0.8}Ni_{0.2}O_{3-\delta}$ ($x \leq 0.3$)

I. Ruiz de Larramendi,[1] R. López Antón,[1,a)] J. I. Ruiz de Larramendi,[1] T. Rojo,[1,b)] A. Wattiaux,[2] and J. Rodríguez Fernández[3]
[1]*Departamento de Química Inorgánica, Facultad de Ciencia y Tecnología, Universidad del País Vasco, Apdo.644, 48080 Bilbao, Spain*
[2]*Institut de Chimie de la Matière Condensée de Bordeaux I.C.M.C.B., C.N.R.S., Université Bordeaux I, 87 Avenue du Docteur Schweitzer 33608, Pessac Cedex, France*
[3]*Fac. Ciencias, CITIMAC, Universidad de Cantabria, 39005 Santander, Spain*

(Received 10 July 2007; accepted 10 November 2007; published online 4 February 2008)

$Pr_{1-x}Sr_xFe_{0.8}Ni_{0.2}O_{3-\delta}$ (x=0.1, 0.2, and 0.3) polycrystalline phases were prepared by combustion synthesis. Their magnetic properties and Mössbauer effect have been examined in the range 5–300 K. Mössbauer spectroscopy shows the existence of charge disproportionation in several of the samples at low temperatures. Meanwhile, the samples present multiple features pointing out a frustrated magnetic order, with competing ferro- and antiferromagnetic interactions. Additionally, exchange bias (EB) phenomena have been observed. Hence, when the samples are cooled in a static magnetic field down to temperatures below 50 K, the hysteresis loops shift in the opposite direction to the applied biasing field, with shifts up to 10 kOe and more, and a small vertical shift of the loops also appears. This behavior seems linked to spin disorder and to the appearance of ferromagnetic (FM) ordered regions at low temperatures when cooling with a high applied field. The growth of these FM regions is likely due to the aligning role of an important cooling magnetic field over Ni-Fe and Fe^{5+}-Fe^{3+} FM interactions. The higher FM contributions and therefore EB values found in the samples presenting charge disproportionation are related to the formation of FM regions in Fe^{5+}-rich areas. © *2008 American Institute of Physics*. [DOI: 10.1063/1.2830984]

I. INTRODUCTION

Since its discovery by Meiklejohn and Bean in 1956,[1] exchange bias (EB) has typically been observed in systems containing ferromagnetic/antiferromagnetic (FM/AFM) interfaces. It manifests itself as a shift, H_E, of the magnetization loop along the field axis when the system is cooled down in an external magnetic field through the Néel temperature of the AFM phase, due to the coupling of the FM phase to the AFM one at the interface.[1] Most EB studies have been done with bilayers of metallic ferromagnets and transition-metal AFM oxides or alloys,[2–4] but it has been also studied in systems involving an interface with a spin glass (SG) phase (e.g., Refs. 5 and 6), and in superstructures of perovskite magnetic oxides.[7,8] EB phenomena have been broadly studied in multilayer systems but also in small particles (e.g., the pioneering works of Meiklejohn and Bean studied Co/CoO particles[1]) and polycrystalline materials (see, e.g., the reviews by Nogues *et al.*[2,9]). In particular, it has also been observed in polycrystalline $La_{1-x}Sr_xCoO_3$,[10] in which there is a spontaneous phase separation FM/SG, and in $SrRuO_3$,[11] which is a SG system. Additionally, Kodama *et al.*[12] and Makhlouf[13] have observed EB in antiferromagnetic NiO and Co_3O_4 nanoparticles, respectively, most likely due to exchange coupling of the frozen moments associated with uncompensated surface spins and the AFM core. However, to date this phenomenon has not been observed in polycrystalline perovskite structure orthoferrites, although they exhibit a fairly broad range of magnetic behaviors. Hence, stoichiometric $SrFeO_3$ is an AFM with a helical magnetic spin structure,[14] whereas in certain oxygen deficient compositions of $SrFeO_{3-\delta}$ a charge ordered state with giant negative magnetoresistance could be observed (due to the Fe^{3+}-Fe^{4+} charge ordering[15]) and also magnetic anomalies associated with a frustrated magnetism.[16] Meanwhile, the $Pr_{1-x}Sr_xFeO_{3-\delta}$ system presents an antiferromagnetic order of type G,[17,18] and charge disproportionation of tetravalent iron,[18] which is also observed in other perovskite oxides as substituted $LaFeO_3$ oxides.[19,20]

On the other hand, perovskite oxides $Ln_{1-x}A_xBO_{3-\delta}$ (Ln=rare earth; A=Sr, Ca, Ba; B=Cr, Mn, Fe, Co, or Ni), exhibit a variety of magnetic and electronic properties. For example, some of these perovskites display good performance as cathode materials in high-temperature solid oxide fuel cells (SOFCs), because of their mixed electronic and ionic conductivity. In particular, the $Pr_{0.7}Sr_{0.3}Fe_{1-x}Ni_xO_{3-\delta}$ series was studied for SOFC cathode material due to the high conductivity showed by these materials[21] and their promising properties as thin films.[22] However, its magnetic properties have not been studied to date.

The present paper reports on the synthesis, structural study, and Mössbauer spectroscopic and magnetic properties of the $Pr_{1-x}Sr_xFe_{0.8}Ni_{0.2}O_{3-\delta}$ (x=0.1, 0.2, and 0.3) series, showing the existence of charge disproportionation in most of the samples and, especially, interesting exchange bias phenomena at low temperatures in all the samples, linked to the

[a)]Currently at Instituto de Ciencia de Materiales de Aragón, CSIC-Universidad de Zaragoza, C/ Pedro Cerbuna 12, 50009 Zaragoza, Spain and ISIS Neutron and Muon Facility, Rutherford Appleton Laboratory, Chilton, Didcot Oxfordshire OX11 0QX, UK.
[b)]Author to whom correspondence should be addressed. Tel: +34 94 6012458, FAX: +34 94 6013500. Electronic mail: teo.rojo@ehu.es.

TABLE I. Nominal and analytical composition of the $Pr_{1-x}Sr_xFe_{0.8}Ni_{0.2}O_{3-\delta}$ samples.

Nominal composition	Analytical composition
$Pr_{0.9}Sr_{0.1}Fe_{0.8}Ni_{0.2}O_3$	$Pr_{0.95}Sr_{0.05}Fe_{0.81}Ni_{0.19}O_{2.99}$
$Pr_{0.8}Sr_{0.2}Fe_{0.8}Ni_{0.2}O_3$	$Pr_{0.80}Sr_{0.13}Fe_{0.78}Ni_{0.16}O_{2.98}$
$Pr_{0.7}Sr_{0.3}Fe_{0.8}Ni_{0.2}O_3$	$Pr_{0.67}Sr_{0.24}Fe_{0.75}Ni_{0.16}O_{2.97}$

existing magnetic disorder and to the formation of FM ordered regions when cooling under a high applied magnetic field.

II. EXPERIMENTAL

Powders of $Pr_{1-x}Sr_xFe_{0.8}Ni_{0.2}O_{3-\delta}$ (x=0.1, 0.2, and 0.3) were prepared according to the combustion synthesis route using glycine as the oxidizing agent. Appropriate amounts of the nitrate salts were dissolved in distilled water; later, glycine was added to the solution. A concentrated gel is formed when the solution is dried and the nitrate-glycine-mixture-gel turns to a vigorous fire, which lasts until the combustion process is completed. The resulting powders were calcined at 800 °C for 10 h in air, then pressed into pellets and calcined again at 1200 °C for 10 h. A portion of the calcined powder sample was randomly collected from a stock batch to perform an analytical analysis of the composition using inductively coupled plasma atomic emission spectroscopy (ICP-AES). In Table I the nominal and analytical composition is shown. In order to estimate the oxygen stoichiometry, the most probable oxidation states for the different cations, as well as a null net electrical charge for the compound, have been taken into account.

The phase purity and the structure of the black polycrystalline powders were checked, at room temperature, by x-ray powder diffraction (powder XRD), using a Philips X'Pert-MPD diffractometer with Cu $K\alpha$ radiation (λ =1.540 60 Å). Refinement of the XRD data by the Rietveld method was carried out using the FULLPROF program.[23]

Magnetization measurements, of the samples in loose powder, were performed in a SQUID magnetometer (Quantum Design MPMS), VSM magnetometer (Cryogenics LTD CFMS), and in a Quantum Design PPMS, the latter used for the ac susceptibility measurements. The temperature range was 5–400 K with applied magnetic fields up to 65 kOe (and up to 120 kOe in the VSM). ^{57}Fe Mössbauer spectra were collected in a HALDER-type spectrometer with constant acceleration and with a ^{57}Co source in a Rh matrix at room temperature. Isomer shifts are expressed with respect to α-iron at 293 K. The samples contain on average 10 mg iron/cm^2, a concentration for which line-broadening effects can be neglected. The spectra were recorded at 293 and 4.2 K using a liquid helium cryostat. The first treatment consists of assuming Lorentzian peaks. In this assumption, the hyperfine parameters (isomer shift, quadrupolar splitting, etc. were refined. A second refinement allowed the analysis of the spectra in terms of quadrupolar splitting distributions or hyperfine field distribution using the method of Hesse *et al.*[24] This method is often used for disordered compounds (environment distributions around iron sites) which give rise to strong line broadening and to line shapes differing from those of a Lorentzian profile. In the second calculation, the isomer shift and the half-height width were fixed as deduced in the first treatment.

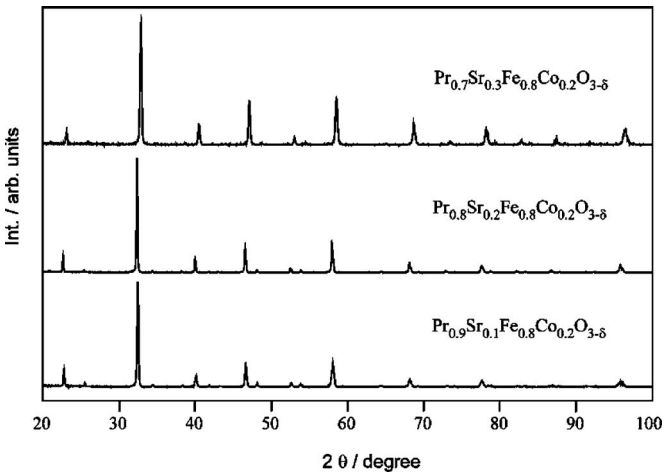

FIG. 1. Powder XRD patterns at room temperature for sintered $Pr_{1-x}Sr_xFe_{0.8}Ni_{0.2}O_{3-\delta}$ (x=0.1, 0.2, and 0.3) samples.

III. RESULTS

A. Crystallographic structure

The powder XRD patterns for $Pr_{1-x}Sr_xFe_{0.8}Ni_{0.2}O_{3-\delta}$ (x =0.1, 0.2, and 0.3) samples are plotted in Fig. 1, whereas the lattice parameters are summarized in Table II. The analysis of these data revealed that the samples are single phase, presenting orthorhombic perovskite structure (space group *Pbnm*), similar to that of $PrNiO_3$ or $PrFeO_3$. Additionally, the unit cell becomes more distorted compared to the ideal cubic perovskite structure as the Sr content is decreased. A preliminary analysis of neutron diffraction data showed that the crystalline structure does not change, nor does a crystallographic phase separation exist at low temperatures.

B. Magnetic measurements

Zero field cooling–field cooling (ZFC-FC) curves, obtained under an applied field of 10 Oe, are shown in Fig. 2. Only the ZFC-FC curves for the $Pr_{0.8}Sr_{0.2}Fe_{0.8}Ni_{0.2}O_{3-\delta}$ and $Pr_{0.7}Sr_{0.3}Fe_{0.8}Ni_{0.2}O_{3-\delta}$ are shown as the ordering temperature of the other sample, $Pr_{0.9}Sr_{0.1}Fe_{0.8}Ni_{0.2}O_{3-\delta}$, was out the temperature range of the SQUID magnetometer. Therefore, for the x=0.1 sample an $M(T)$ curve was obtained in a Faraday magnetometer under an applied field of 6.7 kOe (not shown in the figure). As can be seen, the ordering temperature (obtained as the minimum of the derivative of the FC curve) increases as we reduce the Sr content, from about 170

TABLE II. Lattice parameters of the $Pr_{1-x}Sr_xFe_{0.8}Ni_{0.2}O_{3-\delta}$ samples. The values in brackets show the estimated error in the last significant number.

x	0.1	0.2	0.3
a(Å)	5.4776(12)	5.4855(3)	5.4859(5)
b(Å)	5.5109(11)	5.4925(3)	5.4731(9)
c(Å)	7.7541(10)	7.7544(3)	7.7546(12)

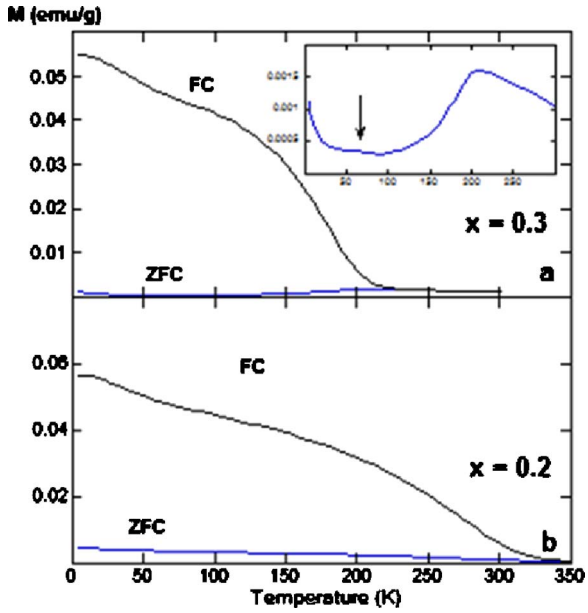

FIG. 2. (Color online) ZFC-FC curves, obtained at 10 Oe, of the samples $Pr_{0.7}Sr_{0.3}Fe_{0.8}Ni_{0.2}O_{3-\delta}$ (a) and $Pr_{0.8}Sr_{0.2}Fe_{0.8}Ni_{0.2}O_{3-\delta}$ (b). Inset: detail of the ZFC curve of the $x=0.3$ sample.

K for the $x=0.3$ sample up to about 470 K for the $x=0.1$ one. Additionally, the FC and ZFC curves bifurcate over the ordering temperature, giving rise to a very large difference between both curves below that temperature. This bifurcation pinpoints the existence of magnetic frustration in the samples. This difference also increases as we obtain the ZFC-FC curves under higher applied fields. In both FC curves there is a small slope change of about 70 K but, additionally, in the case of the $x=0.3$ sample we also find a small bump in the ZFC curve at the same temperature (as can be seen in the detail of Fig. 2), which is not observed in the other samples.

In Fig. 3 we show the ac susceptibility (real part, χ', and imaginary, χ'') for the samples with $x=0.2$ and 0.3, obtained

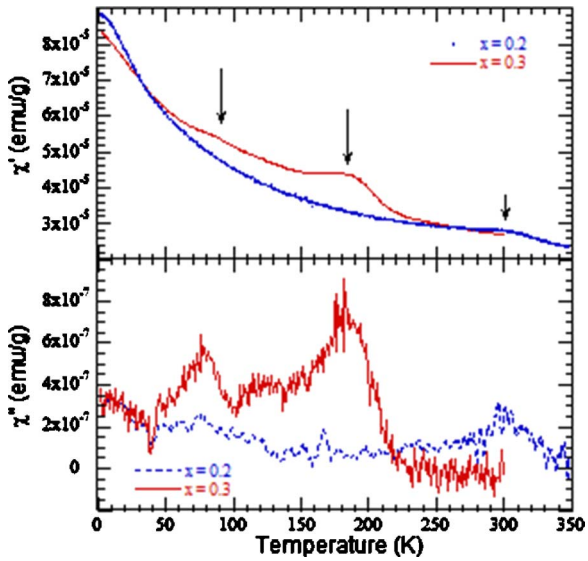

FIG. 3. (Color online) Real part χ' and imaginary part χ'' of the ac susceptibility of the $x=0.2$ and 0.3 samples (measured with a frequency of 1 kHz and ac applied field of 1 Oe).

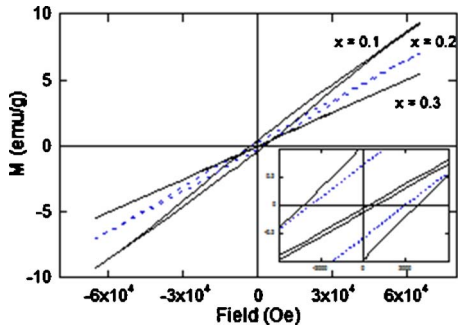

FIG. 4. (Color online) Hysteresis loops, obtained at 5 K and cooled without applied field, of the $Pr_{1-x}Sr_xFe_{0.8}Ni_{0.2}O_{3-\delta}$ ($x=0.1$, 0.2, and 0.3) samples. The inset shows an enlargement of the loops at low fields.

at 1 kHz and 1 Oe of the ac field. With regard to the χ', a weak peak is found at about 300 K for the $x=0.2$ sample, which corresponds to the ordering temperature observed in the ZFC-FC curve and is indicated by a short arrow in Fig. 3. Meanwhile, in the case of the χ'', which is very sensitive to any dynamical magnetic process, the peaks corresponding to the ordering temperature are clearly seen. In addition, for the $x=0.3$ sample, the bump observed in the χ' at 70 K transforms into a peak in the χ'', which clearly demonstrates the existence of some kind of magnetic transition at this temperature.

The magnetic loops obtained at 5 K after cooling without an applied field are shown in Fig. 4. All of them are quite linear, nonsaturating even at 65 kOe, and with a certain hysteresis which decreases as we increase the quantity of Sr in the samples (hence, the loop of the $x=0.1$ sample is quite broad, while on the contrary that of the $x=0.3$ sample is fairly narrow—see the inset of Fig. 4). These hysteresis loops are not totally centered but slightly displaced in the applied field axis. This tendency could be associated with the coexistence of antiferromagnetic and ferromagnetic interactions[16,25] and is typical in materials with helical magnetic ordering.[26] However, this shift of the loop, related to the coexistence of different magnetic interactions, is also a hint of a possible exchange bias, so the $x=0.2$ and 0.3 samples were therefore measured at 5 K but cooled with different fields (up to 65 kOe) from temperatures above the ordering temperature, as can be observed in Fig. 5. Quite a different behavior is found between the samples: for the x

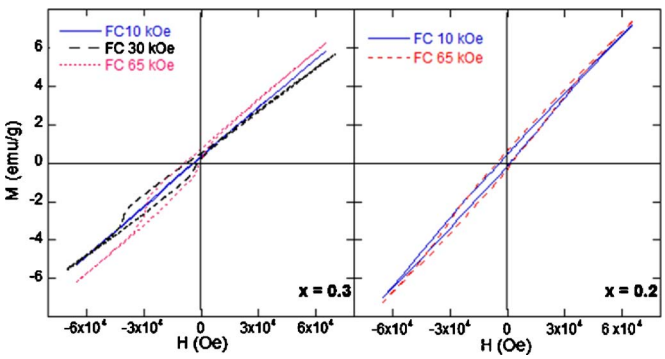

FIG. 5. (Color online) Hysteresis loops of the $x=0.2$ and $x=0.3$ samples at low temperature cooled under different applied fields. The loops were obtained at 5 K excepting the one for the $x=0.3$ sample, 30 kOe (at 2.5 K).

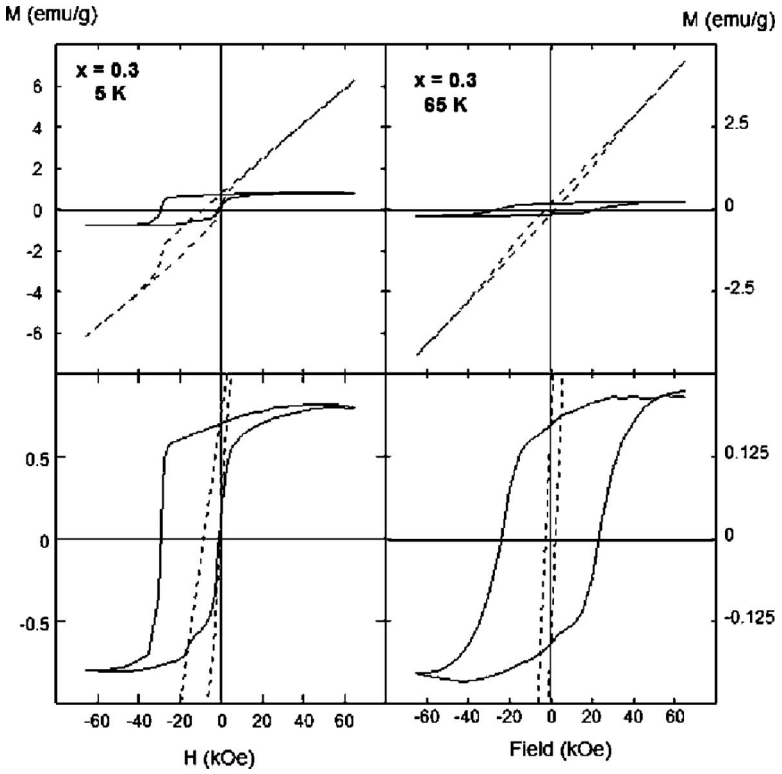

FIG. 6. Hysteresis loop of the $Pr_{0.7}Sr_{0.3}Fe_{0.8}Ni_{0.2}O_{3-\delta}$ sample at 5 K (left) and 65 K (right) after cooling under an applied field of 65 kOe, before (dashed line) and after (continuous line) subtracting a linear contribution from the loop. The low figures show detail, focusing on the hysteresis loops after subtracting the linear contribution.

=0.2 sample, the shape of the hysteresis loop is always the same, although it broadens and shifts (i.e., the coercive field and the shift augment) as we increase the applied magnetic field. This trend is also observed for the $x=0.1$ sample. On the other hand, for the $x=0.3$ one, the loops show the same trend as the other samples with cooling fields up to 10 kOe (though the loops are narrower) but, with cooling fields equal to or higher than 30 kOe, a manifest change of its shape occurs, appearing as an evident hysteresis (with high coercivities and important magnetic remanences) in addition to a very large exchange bias (EB). Nevertheless, there is still a linear contribution which avoids magnetic saturation even at 70 kOe (Fig. 5). Several additional measurements were performed in a VSM with even higher fields (up to 120 kOe), but the behavior observed was the same.

In order to compare the evolution of the observed shift with the temperature, hysteresis loops have been obtained at different temperatures after cooling from temperatures above the ordering temperature (or from 400 K for the $x=0.1$ sample) with an applied field during cooling of 65 kOe. In all the cases the linear contribution was removed from the loops in order to remove the AFM contribution and focus on the hysteretic contribution. Two of the loops before and after removing this linear contribution are shown in Fig. 6, whereas the evolution of the coercive field and the exchange bias with the temperature is shown in Fig. 7. It can be observed that this non-AFM contribution is fairly smaller (about one order of magnitude) than the AFM one. This contribution is maximum at 5 K for all the samples and decreases with increasing temperature, strongly up to about 50 K and then with a gentler slope after that temperature. In particular, the $x=0.3$ sample presents the higher ratio between this contribution and the total magnetization, coupled with non-negligible changes in the shape of the loops as we approach 70 K (in the other samples there are also changes in the shape but not as strong). Several of the loops are open up to the maximum applied field (especially for the cases in which the coercive field is high). In several cases in which the loops are open and indeed are minor loops, this fact can induce an artifact similar apparently to a fake EB.[27–29] Nevertheless, in our case, given the high magnetic field used and the additional measurements at even higher fields where a higher EB was observed (in contrary to what would be expected with this type of artifact), it does seem to be the case (and if there is such an artifact, its effect is fairly small compared with the real one). On the other hand, for temperatures higher than 50 K (i.e., exactly when the EB practically disappears) the two branches, the descending and ascending ones, cross, i.e., the ascending one reaches a higher final value than the one from which the descending branch started

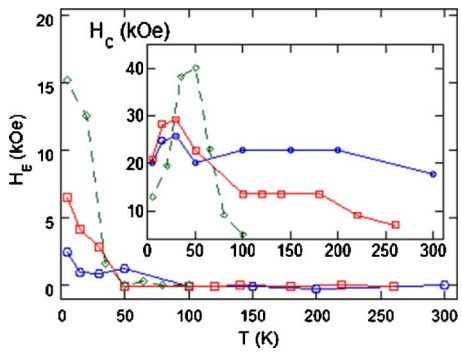

FIG. 7. (Color online) Evolution of the exchange bias, H_E, and coercive field H_C (detail) with the temperature after cooling down under an applied field of 65 kOe for the $x=0.1$ (circles), $x=0.2$ (squares), and $x=0.3$ (diamonds) samples.

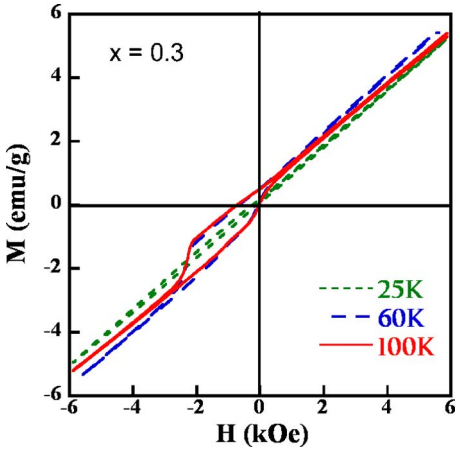

FIG. 8. (Color online) Hysteresis loops of the $x=0.3$ sample at 5 K cooled under 65 kOe from different temperatures.

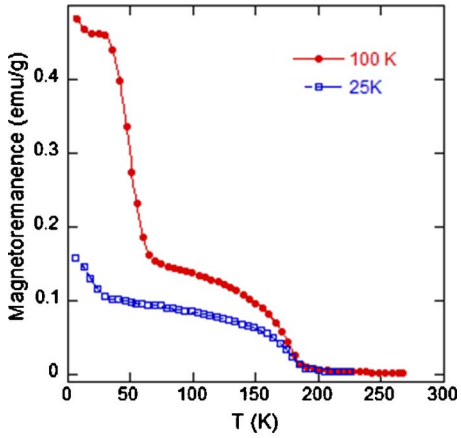

FIG. 9. (Color online) Thermoremanence of the $x=0.3$ sample after cooling under an applied field of 65 kOe from 100 and 25 K.

(as can be seen in Fig. 6). This behavior only happens when we cool the samples under a high magnetic applied field. Additionally, there is also a small vertical shift in the loops, reaching higher values for the $x=0.1$ sample, which is usually associated with the presence of uncompensated spins at the interface between different magnetic media.[30,31]

The coercive field exhibits a maximum at low temperatures, decreasing afterwards. This peak of the coercive field close to the temperature where the exchange bias disappears brings to mind the work of Leighton *et al.*,[32] who observed such a peak close to the Néel temperature in FM/AFM multilayers when the ratio of the F layer thickness compared to the AFM one is bigger than a particular value. For the $x=0.3$ sample the decrease is very sharp, whereas for the $x=0.1$ the coercive field remains about 20 kOe up to 300 K. Meanwhile, the exchange bias is only present at low temperature, being maximum at 5 K and decreasing with increasing temperature up to 50–100 K, where it disappears. The temperature when the EB vanishes is fairly close to the one in which a peak was observed in the ZFC and ac measurements of the $x=0.3$ sample, and also where the $x=0.2$ one had a change of slope in the FC curve, evidencing a certain transition at that temperature. The exchange bias is bigger for the $x=0.3$ sample and decreases strongly as the percentage of Sr is reduced. In the case of the $x=0.1$ sample, the EB values are fairly smaller but also the decrease is smoother.

Given the behavior of the sample $x=0.3$, hysteresis loops at 5 K after cooling from different temperatures under an applied field of 65 kOe have been performed (Fig. 8). When cooled down from 25 K (well below the observed threshold temperature for the exchange bias), the loop is very linear and with a small hysteresis, quite similar to the ones obtained when cooling from higher temperatures but without enough field. Meanwhile, when cooling from 60 K onwards, the loop obtained is similar to that shown in Fig. 5, with a very evident exchange bias and a well-marked hysteresis.

Measurements of the thermoremanence for the sample $x=0.3$ are shown in Fig. 9, after cooling under an applied field of 65 kOe from 100 and 25 K. When cooling from 100 K, a small decrease is observed as the temperature increases up to about 20 K, a little plateau afterwards, and then a sharp decrease centered at 50 K. This sharp decrease ends at about 70 K. After that, the thermoremanence keeps on decreasing, although with a fairly smaller slope up to the ordering temperature, where it decreases more abruptly toward zero. Meanwhile, when it is cooled from 25 K, we reach a fairly smaller remanence at low temperatures, without the previously observed plateau up to 50 K, indicating that we have not been able to enhance the FM interactions as strongly as when it is cooled from 100 K.

C. Mössbauer spectroscopy

Figures 10 and 11 show the Mössbauer spectra obtained at 4.2 and 293 K, respectively, whereas the obtained Mössbauer parameters are summarized in Table III. It is noteworthy that, for all the compositions, the width of the distributions indicates the important existing disorder around Fe sites due to the presence of three cations (Ni, Sr, and Pr). The compounds are therefore heterogeneous in composition. At 293 K we are above the ordering temperature of the $x=0.3$ sample, slightly below that temperature for the $x=0.2$ one, and quite below it for the $x=0.1$ one, in agreement with the magnetic measurements. Therefore, in the $x=0.3$ sample only paramagnetic contributions exist, whereas for the other two both PM and AFM contributions are observed. In the $x=0.1$ sample, only Fe^{3+} is found, in three different sites, likely due to a random distribution of Sr and Pr in the A sites and Ni ions at the B sites. It should be noted that one of these sites exhibits no magnetically ordered behavior, though we are quite far from the ordering temperature. This does not seem to be a superparamagnetic effect as we do not have such small grains. It could be linked hence to the existence of Sr^{2+}-rich domains which could affect the behavior of the Fe^{3+}. As we increase x, Fe^{4+} starts to appear, increasing from 7% for the $x=0.2$ to 13% for the $x=0.3$ one. This is logical: as the Sr^{2+} content is augmented, the Fe^{4+} content must also increase in order to keep the charge. The absence of Fe^{4+} in the $x=0.1$ sample could be explained taking into account the very small concentration of Sr (about 0.05 according to the ICP analysis), giving rise to such a tiny Fe^{4+} content that it is difficult to discern, whereas the lower than expected value in

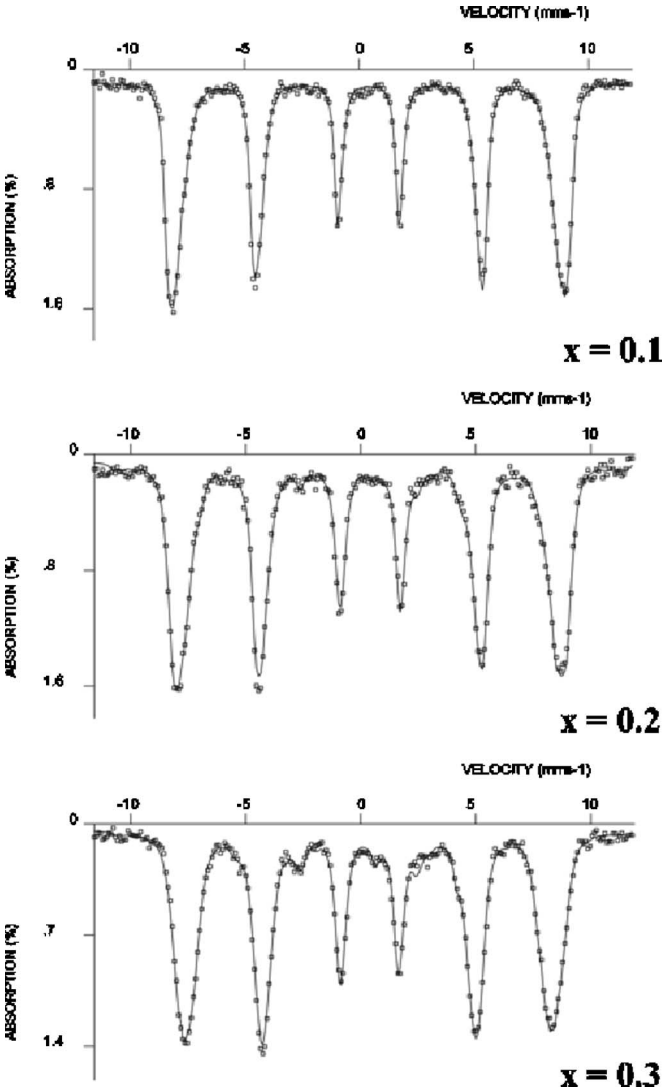

FIG. 10. Mössbauer spectra of $Pr_{1-x}Sr_xFe_{0.8}Ni_{0.2}O_{3-\delta}$ (x=0.1, 0.2, and 0.3) samples collected at 4.2 K.

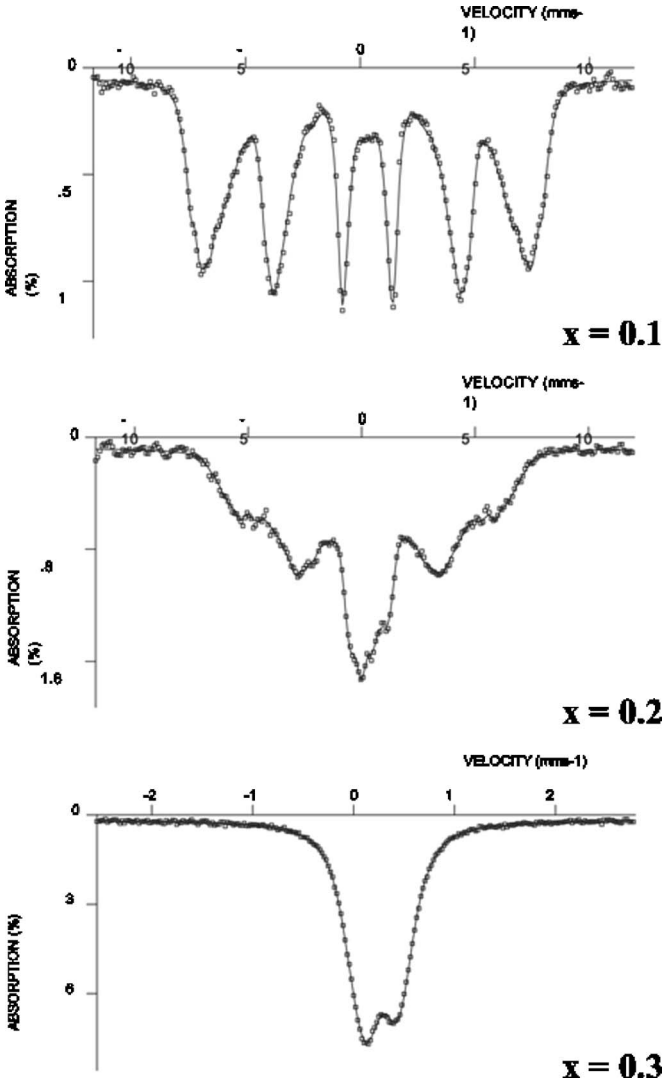

FIG. 11. Mössbauer spectra of $Pr_{1-x}Sr_xFe_{0.8}Ni_{0.2}O_{3-\delta}$ (x=0.1, 0.2, and 0.3) samples collected at 293 K.

the other two samples could be due to the existence of a certain amount of $Fe^{(3+n)+}$ ions. Also noteworthy is the isomer shift (IS) value of 0.29 mm/s found in the x=0.3 sample for the Fe^{3+} ion, slightly lower than the values observed in the literature for similar ferrites (and also in the other studied samples),[33,34] which is likely linked to the existence of $Fe^{(3+n)+}$ ions (n about 0.20, as estimated from the IS value) instead of just Fe^{3+} ions.

At 4.2 K only sextets are found, without any paramagnetic contribution (as could be expected). In all the cases Fe^{3+} is found but in some of the samples (x=0.2, 0.3) a sextet also appears with an IS of −0.03 mm/s and a hyperfine field of about 26 T, common values for Fe^{+5}. However, the appearance of this Fe^{5+} ion does not satisfy the disproportionation reaction observed by other authors,[18–20,35,36]

$$2Fe^{4+} \rightarrow Fe^{3+} + Fe^{5+}. \quad (1)$$

This could be explained by a reaction in which, in addition to the Fe charge disproportionation, Ni also suffers a certain change of oxidation at low temperature, in a similar way to the observed change of oxidation state of Co coupled with the Fe charge disproportionation by Pedersen *et al.* in $(Ln_{0.6}Sr_{0.4})_{0.99}Fe_{0.8}Co_{0.2}O_{3-d}$.[33] On the other hand, given the fact that in the sample x=0.3 we have $Fe^{(3+n)+}$ instead of just Fe^{3+}, at room temperature these $Fe^{(3+n)+}$ can also contribute to the charge disproportionation according to the equations

$$Fe^{(3+n)+} \rightarrow (1-n)Fe^{3+} + nFe^{4+} \quad (293\ \text{K}), \quad (2a)$$

$$n\ Fe^{4+} \rightarrow (n/2)Fe^{3+} + (n/2)Fe^{5+} \quad (4.2\ \text{K}), \quad (2b)$$

which could explain quite well the obtained values [using Eqs. (1), (2a), and (2b) with n=0.20, we should have 15% of Fe^{+5} at low temperature, not very far from the experimentally obtained value of 14]. In the case of the x=0.2 sample, the isomer shifts observed at room temperature were not as low, so it does not seem as evident that we have $Fe^{(3+n)+}$ in that case. However, for the observed quantity of Fe^{5+} at low temperature, just a small percentage of $Fe^{(3+n)+}$ in each position (with small n values, lower than 0.10) should be necessary (e.g., with percentages about 25–35% and n values between 0.07 and 0.09 in addition to the existing Fe^{4+} we would obtain the measured Fe^{5+} and a very small change should occur in the hyperfine parameters, if any). Hence, we think this is the explanation of this behavior in our samples.

TABLE III. Hyperfine parameters, relative intensity (%), valence state, and Fe sites observed in ^{57}Fe Mössbauer spectra obtained at 4.2 and 293 K. The isomer shift (δ) and the quadrupole shift (ε) have been obtained from the initial fit, while the mean quadrupole splitting (Δ) and the mean hyperfine field (H_f) of the respective distributions have been obtained from the second refinement.

x	T(K)	δ(mm/s)	ε(mm/s)	Δ(mm/s)	H_f(T) (± 2 T)	% (± 2 %)	Valence state
0.10	4.2	0.46	0.01		52.6	87	$Fe^{3+}O_h$
		0.44	−0.25		52.6	13	$Fe^{3+}O_h$
	293	0.348	−0.031		40.7	37	$Fe^{3+}O_h$
		0.354	−0.025		41.3	52	$Fe^{3+}O_h$
		0.35		2.19		11	$Fe^{3+}O_h$
0.20	4.2	0.47	−0.15		50.8	20	$Fe^{3+}O_h$
		0.44	0.01		52.2	72	$Fe^{3+}O_h$
		−0.03	0.001		25.4	8	Fe^{5+}
	293	0.348	−0.031		26.5	35	$Fe^{3+}O_h$
		0.354	−0.025		29.5	31	$Fe^{3+}O_h$
		0.35		0.94		27	$Fe^{3+}O_h$
		0.01		0.55		7	$Fe^{4+}O_h$
0.30	4.2	0.43	−0.20		48.8	16	$Fe^{3+}O_h$
		0.41	0.01		50.3	70	$Fe^{3+}O_h$
		−0.03	0.001		27.6	14	Fe^{5+}
	293	0.29		0.33		87	$Fe^{(3+n)+}O_h$
		0.01		0.11		13	$Fe^{4+}O_h$

IV. DISCUSSION

Several trends in the magnetic behavior, for example, the hysteresis loops obtained at low temperature after cooling without applied field or the ZFC-FC curves, pinpoint a certain magnetic frustration in our samples. It should be recalled that the $Pr_{1-x}Sr_xFeO_{3-\delta}$ system exhibits an antiferromagnetic order of type G with varying amounts of frustrated spins.[17,18] The inclusion of Ni ions at the B position, as it is our case, harasses/breaks the long-range order, creating smaller AFM domains and increasing the magnetic frustration and spin disorder. Additionally, the partial substitution of Pr by Sr in the A site induces a mixed valence of Fe, which is also subject to a charge disproportionation at low temperatures, complicating the magnetic frame of our system even more.

On the other hand, exchange bias phenomena are observed in all the samples at low temperature. As we have commented previously, the microscopic exchange interaction at the contact interfaces between ferromagnetic (FM) and antiferromagnetic (AFM) of a material, after it has been cooled down in a magnetic field through the Néel temperature of the AFM phase, is believed to be responsible for the horizontal shift of the loop observed in EB phenomena.[1,9,37] Nevertheless, EB has been observed also in other systems, with FM/SG phase separation,[10,38] with just a SG phase,[11] or with AFM nanoparticles[6,12,13] due to spin disorder in their surface. In the case of the $Pr_{1-x}Sr_xFe_{0.8}Ni_{0.2}O_{3-\delta}$ samples, the situation is a little bit complicated, as we have commented. On the one hand, EB is likely partly related to spin-disorder zones and AFM domains given the so important magnetic frustration found in the samples. In fact, the observed loops when cooling under a magnetic field, especially for the $x=0.1$ and 0.2 samples, are more similar to the ones found by Makhlouf *et al.* in AFM nanoparticles,[12,13] which have a very important spin disorder in their surface. However, in contrast to the Co_3O_4 nanoparticles studied by Makhlouf,[13] which showed an important EB up to the Néel temperature, our samples only present it under about 50 K, well below the ordering temperature. On the other hand, part of their behavior could be explained by the existence of FM ordered regions in addition to the AFM ones (already divided into domains). In fact, it seems that through cooling with high fields it is possible to induce such regions in these samples, as is evidenced by the loops observed (see Figs. 5 and 6), the evolution of the thermoremanence for the sample $x=0.3$ (Fig. 8) being especially more evident for the sample $x=0.3$. It is as if, when cooling with these fields, we are able to ferromagnetically align several regions in which the FM interactions were the most important, overcoming the AFM interactions locally. The EB appears at about 50–70 K, at exactly the same point in which there is also a change in the hysteresis loops (slightly open loops right below that temperature and with crossed branches over it), pinpointing that at this temperature a better ordering of these FM regions is reached and then they also contribute to the exchange bias phenomena. Also at this temperature the ZFC-FC curve and the ac susceptibility showed a certain bump for the $x=0.3$ sample (and there was a certain change of slope in the FC curve for the $x=0.2$ one), which stresses the idea that some kind of transition happens at that point. Nevertheless, the evolution of the EB with the temperature or with the cooling field is not exactly as the one found for other FM/AFM systems with a Curie temperature below or close to the Néel one,[39–41] as it seems could be our case, probably due to the additional spin disorder and AFM domains existing.

These FM ordered regions could be related to the appearance of FM interactions of the Fe with the Ni and to the appearance of Fe^{5+} at low temperatures in the $x=0.2$ and $x=0.3$ samples (which interestingly presents a moderate ferromagnetic interaction with a high state Fe^{3+} via oxygen by the superexchange mechanism[41]). This extra contribution linked

to the Fe^{5+} presence could explain why these two samples, which have a charge disproportionation, present a higher ratio of FM contribution compared with the AFM one and also fairly bigger exchange values at low temperatures. In this sense, the $x=0.3$ sample is the one in which the evidences for the FM ordering are more marked (indeed, its hysteresis loops are more prominently changed when cooling with a high field, evident even without removing the linear AFM contribution) and that is why we have made additional measurements, as thermoremanence or the evolution of the loops when field cooling from different temperatures. This agrees well to the fact that is the sample with the greater proportion of Fe^{5+} (with its FM interaction with Fe^{3+}) is found at low temperatures, giving place to several of the regions presenting FM behavior after cooling under a field. Additional measurements are required in order to better understand the complicated magnetic behavior of these samples and the mechanism giving rise to the formation of FM ordered regions when cooling under a high field, so neutron diffraction and Mössbauer spectroscopy measurements are underway in that sense.

V. CONCLUSIONS

The magnetic properties and Mössbauer effect of $Pr_{1-x}Sr_xFe_{0.8}Ni_{0.2}O_{3-\delta}$ ($x=0.1$, 0.2, and 0.3) polycrystalline phases have been examined. Mössbauer spectroscopy shows the existence of charge disproportionation in several of the samples at low temperatures. From the magnetic point of view, the samples present a frustrated magnetic order, with competing ferro- and antiferromagnetic interactions. Exchange bias phenomena, with horizontal shifts of the loops even over 10 kOe, and small vertical shifts, have been observed which seem linked to the appearance of FM ordered regions at low temperatures and to the spin disorder existing in the samples. The formation of these FM regions is probably due to the aligning role of an important cooling magnetic field over Ni-Fe and Fe^{5+}-Fe^{3+} FM interactions. This last mechanism, linked to Fe^{5+}-Fe^{3+} FM interactions, explains the higher FM contributions and therefore EB values found in the samples presenting charge disproportionation.

ACKNOWLEDGMENTS

This work has been partially financed by the Spanish CiCyT under Project MAT2004-02425 and MAT2007-66737-C02–01 and by the University of the Basque Country under Project UPV/EHU: GIU06/11. I. Ruiz de Larramendi thanks the Eusko Jaurlaritza/Gobierno Vasco for her predoctoral fellowship, and R.L.A. thanks the Spanish CiCyT for funding his research activities as postdoc within Project MAT2004-02425. We are indebted to Dr. I. Orue, from the SGIker (EHU-UPV), for his help in the magnetic characterization and enlightening discussions.

[1]W. H. Meiklejohn and C. P. Bean, Phys. Rev. **102**, 1413 (1956).
[2]J. Nogués and I.K. Schuller, J. Magn. Magn. Mater. **192**, 203 (1999), and references therein.
[3]J. S. Kouvel, J. Phys. Chem. Solids **24**, 795 (1963).
[4]B. Dieny, V. S. Spirous, S. S. P. Parkin, B. A. Gurney, D. R. Wilhoit, and D. Maury, Phys. Rev. B **43**, 1297 (1991).
[5]R. H. Kodama, A. E. Berkowitz, E. J. McNiff, and S. Foner, Phys. Rev. Lett. **77**, 394 (1996).
[6]B. Martinez, X. Obradors, Ll. Balcells, A. Rouanet, and C. Monty, Phys. Rev. Lett. **80**, 181 (1998).
[7]I. Panagliotopoulos, C. Christides, N. Moutis, M. Pissas, and D. Niarchos, J. Appl. Phys. **85**, 5484 (1999).
[8]X. Ke, M. S. Rzchowoski, L. J. Belenky, and C. B. Eom, Appl. Phys. Lett. **84**, 5458 (2004).
[9]J. Nogues, J. Sort, V. Langlais, V. Skumryev, S. Suriñach, J.S. Muñoz, and M.D. Baro, Phys. Rep. **422**, 65 (2005), and references therein.
[10]Y. K. Tang, Y. Sun, and Z-H. Cheng, Phys. Rev. B **73**, 174419 (2006).
[11]L. Pi, S. Zhang, S. Tan, and Y. Zhang, Appl. Phys. Lett. **88**, 102502 (2006).
[12]R. H. Kodama, S. A. Makhlouf, and A. E. Berkowitz, Phys. Rev. Lett. **79**, 1393 (1997).
[13]S. A. Makhlouf, J. Magn. Magn. Mater. **246**, 184 (2002).
[14]T. Takeda, Y. Yamaguchi, and H. Watanabe, J. Phys. Soc. Jpn. **33**, 967 (1972).
[15]A. Lebon, P. Adler, C. Bernhard, A. V. Boris, A. V. Pimenov, A. Maljuk, C. T. Lin, C. Ulrich, and B. Keimer, Phys. Rev. Lett. **92**, 037202 (2004).
[16]S. Srinath, M. Mahesh Kumar, M. L. Post, and H. Srikanth, Phys. Rev. B **72**, 054425 (2005).
[17]H. W. Brinks, H. Fjellvåg, A. Kjekshus, and B. C. Hauback, J. Solid State Chem. **150**, 233 (2000).
[18]M. Stange, J. Linden, A. Kjekshus, N. Binsted, M. T. Weller, B. C. Hauback, and H. Fjellvåg, J. Solid State Chem. **173**, 148 (2003).
[19]J. B. Yang, X. D. Zhou, Z. Chu, W. M. Hikal, Q. Cai, J. C. Ho, D. C. Kundaliya, W. B. Yelon, W. J. James, H. U. Anderson, H. H. Hamdeh, and S. K. Malik, J. Phys.: Condens. Matter **15**, 5093 (2003).
[20]U. Russo, L. Nodari, M. Faticanti, V. Kuncser, and G. Filoti, Solid State Ionics **176**, 97 (2005).
[21]S.-I. Hashimoto, K. Kammer, P. H. Larsen, F. W. Pulsen, and M. Mogensen, Solid State Ionics **176**, 1013 (2005).
[22]I. Ruiz de Larramendi, R. López Antón, J. I. Ruiz de Larramendi, S. Baliteau, F. Mauvy, J. C. Grenier, and T. Rojo, J. Power Sources **169**, 35 (2007).
[23]J. Rodríguez-Carvajal, Physica B (Amsterdam) **55**, 192 (1993); J. Rodríguez-Carvajal, *FULLPROF Program: Rietveld Pattern Matching Analysis of Powder Patterns* (ILL, Grenoble, 1994).
[24]J. Hesse and A. Rubartsch, J. Phys. E **7**, 526 (1974).
[25]S. Srinath, M. Mahesh Kumar, K. Sahner, M.L. Post, M. Wickles, R. Moos, and H. Srikanth, J. Appl. Phys. **99**, 08S904 (2006).
[26]K. Kadowaki, K. Okuda, H. Kuwahara, Y. Morimoto, and Y. Tokura, J. Phys. Soc. Jpn. **51**, 2433 (1982).
[27]J. Geshev, J. Magn. Magn. Mater. **316**(2), e97 (2007).
[28]B. D. Cullity, *Introduction to Magnetic Materials* (Addison-Wesley, London, 1972).
[29]G. Salazar-Alvarez, J. Sort, S. Suriñach, M. D. Baro, and J. Nogues, J. Am. Chem. Soc. **129**, 9102 (2007).
[30]H. Ohldag, A. Schll, F. Nolting, E. Arenholz, S. Maat, A. T. Young, M. Carey, and J. Stohr, Phys. Rev. Lett. **91**, 017203 (2003).
[31]O. Iglesias, X. Batle, and A. Labarta, Phys. Rev. B **72**, 212401 (2005).
[32]C. Leighton, M. R. Fitzsimons, A. Hoffman, J. Dura, C. F. Majkrzak, M. S. Lund, and I. K. Schuller, Phys. Rev. B **65**, 064403 (2002).
[33]T. Pedersen, S. Saadi, K. H. Nielsen, S. Mørup, and K. Kammer, Solid State Ionics **176**, 1555 (2005).
[34]P. Adler, A. Lebon, V. Damljanović, C. Ulrich, C. Bernhard, A. V. Boris, A. Maljuk, C. T. Lin, and B. Keimer, Phys. Rev. B **73**, 094451 (2006).
[35]P. Adler, J. Solid State Chem. **130**, 129 (1997).
[36]K. Kuzushita, S. Morimoto, S. Nasu, and S. Nakamura, J. Phys. Soc. Jpn. **69**, 2767 (2000).
[37]E. C. Passamani, C. Larica, C. Marques, J. R. Proveti, A. Y. Takeuchi, and F. H. Sanchez, J. Magn. Magn. Mater. **299**, 11 (2006).
[38]J. Blasco, J. Stankiewicz, and J. Garcia, J. Solid State Chem. **179**, 898 (2006).
[39]X. W. Wu and C. L. Chien, Phys. Rev. Lett. **81**, 2795 (1998).
[40]J. W. Cai, K. Liu, and C. L. Chien, Phys. Rev. B **60**, 72 (1999).
[41]J. B. Goodenough, *Magnetism and the Chemical Bond* (Wiley-Interscience, New York, 1963).